

## 第 2 章 臨時地震観測による余震活動調査

### 2. 2

Aftershock distribution and 3D seismic velocity structure in and around the focal area of the 2004 mid Niigata prefecture earthquake obtained by applying double-difference tomography to dense temporary seismic network data

T. Okada, N. Umino, T. Matsuzawa, J. Nakajima, N. Uchida, T. Nakayama, S. Hirahara, T. Sato, S. Hori, T. Kono, Y. Yabe, K. Ariyoshi, S. Gamage, J. Shimizu, J. Suganomata, S. Kita, S. Yui, M. Arao, S. Hondo, T. Mizukami, H. Tsushima, T. Yaginuma, A. Hasegawa

Research Center for Prediction of Earthquakes and Volcanic Eruptions, Graduate School of Science, Tohoku Univ

Y. Asano.

National Research Institute for Earth Science and Disaster Prevention

H. Zhang, C. Thurber

Department of Geology and Geophysics, University of Wisconsin-Madison

#### **Abstract**

A destructive large earthquake (the 2004 mid Niigata prefecture earthquake) sequence occurred in the central part (Chuetsu district) of Niigata prefecture, central Japan on October 23, 2004. We have deployed a temporary seismic network composed of 54 stations for aftershock observation just above and around the focal area of the earthquake for about a month. Using travel time data from the temporary seismic network and surrounding routine stations, we obtained precise aftershock distribution and 3D seismic velocity structure in and around the fault planes of the earthquake and four major ( $M \geq 6$ ) aftershocks by double-difference tomography. The results clearly show three major aftershock alignments. Two of them are almost parallel and dipping toward the WNW. The shallow and deep aftershock alignments correspond to the fault

plane of the mainshock and that of the largest aftershock (M6.4), respectively. The third alignment is almost perpendicular to the WNW-ward dipping planes and perhaps corresponds to the fault plane of the M6 aftershock on October 27. General feature of the obtained velocity structure is that the hanging wall (western part of the focal area) has lower velocity and the footwall (eastern part of the focal area) has higher velocity. Major velocity boundary seems to shift westward in comparison to in northern and southern parts at a location near the central part of the focal area, where the main shock rupture started. Some parts of the fault planes were imaged as low velocity zones. This complex crustal structure would be one of possible causes of the multi-fault rupture of the 2004 mid Niigata prefecture earthquake sequence. (Earth, Planets and Space / Special section for the 2004 Mid Niigata Prefecture Earthquake, in press, 2005)

## Introduction

A destructive large earthquake with a magnitude of 6.8 and many aftershocks occurred in the central part (Chuetsu district) of Niigata Prefecture, Central Japan on October 23, 2004. In this earthquake sequence, four M6-class aftershocks occurred. Focal mechanisms of most of moderate-sized or large events (e.g. F-Net, NIED, 2005) in this sequence are reverse fault-types. This earthquake sequence is located just to the northwest of the Muikamachi fault and thought to have occurred along the Shinano-river active fold and thrust zone (e.g. Kim and Okada, 2005, Kim et al., 2005). To improve the accuracy of hypocenter locations and to obtain more detailed information about the present earthquake sequence, we deployed a dense temporary seismic network composed of 54 stations with data loggers just above and around the focal area after the occurrence of the earthquake. In this study, we performed seismic tomography to acquire detailed aftershock distribution and seismic velocity structure in and around the focal area of the 2004 mid Niigata prefecture earthquake based on data obtained by this seismic network.

## Observation

We deployed a temporary seismic network of 54 stations in and around the focal area of the present earthquake (Fig. 1). Signals of 3 components of 2Hz seismographs are continuously recorded at a sampling rate of 100Hz. We used the LS8000 logger (Hakusan Co. Ltd.:AD 22bits) at 21 stations and the DAT-2GC (Clovertech Co. Ltd.:AD

16bits) at the other 31 stations. The loggers were powered by car batteries. Clock in the data logger is calibrated by GPS clock in an interval of a few hours; the timing error in sampling is less than 0.1 msec. The observation started on October 25 and lasted until November 27.

## Method & Data

For the present analysis, we adopted the double-difference (DD) tomography method (Zhang and Thurber, 2003). This method uses not only absolute travel times but also travel time differences between nearby events at each station and has the advantage of obtaining the seismic velocity structure at high spatial resolution for areas where hypocenters are densely distributed such as aftershock areas.

The shallow structure of the focal area of the present event is expected to be complex due to fold and thrust structure as previously pointed out in a report on the 1995 northern Niigata earthquake (M6.0) (Sakai et al., 1995), which occurred about 80km northeast from the present earthquake. It is better to use a plausible starting velocity structure and hypocenter locations for tomographic inversions on three-dimensional seismic velocity structure at such complex structure (Kissling et al., 1994). First, we located hypocenters of aftershocks individually. The seismic velocity model routinely used in the Tohoku University seismic network, which is thought to represent the typical structure in northeastern Japan (Hasegawa et al., 1978), was adopted in the calculation of travel times. Then, we relocated hypocenters and determine station corrections of individual stations and one-dimensional velocity structure simultaneously. Finally we determined hypocenters and three-dimensional velocity structure by DD tomography. Note that in this final stage, we used hypocenters determined by using station corrections as `initial` hypocenters, but we used original arrival times in the inversion procedure.

We used arrival time data picked manually at the temporary stations and those at surrounding routine stations of Tohoku University, Univ. of Tokyo, JMA, and Hi-net with epicentral distances of less than 60 km. In total, 107 stations were used. We relocated 2544 events that occurred in the period from October 27 to November 21 and were located by JMA. Although the main shock and three M6-class aftershocks on October 23 had occurred before we deployed the temporary seismic network, we add travel time data observed at surrounding routine stations for these events and relocate them simultaneously. There were 701,076 P-wave and 499,554 S-wave arrival-time pairs for calculating travel time differences, and 85,606 P-wave and 69,596 S-wave arrivals. Grid intervals are 2km and 4km in the central part of the focal area and in the

surrounding area, respectively.

## Results

Figure 2 shows P-wave velocity distribution at a depth of 4km. We could determine reliable seismic velocity structure in and around the focal area with a width of about 20km, where derivative weighted sum (DWS; Thurber and Eberhart-Phillips, 1999, i.e. the sum of partial derivatives of travel times with respect to slowness at each grid and an indicator how the data are sensitive to the change in the velocity at the grid.) values are high and reliable resolutions for assumed grid size can be obtained. General feature is that the hanging wall (western part of the focal area) has lower velocity and the footwall (eastern part of the focal area) has higher velocity. This feature is clearly observed in the southern part of the focal area, but, less clear in the northern part. In the central part, higher velocity areas overhang to the west and the major velocity boundary seems to shift westward in comparison to in northern and southern parts.

Figures 3 to 5 show vertical cross sections of hypocenters and seismic velocities across the main shock fault (Strike: N120E). Origin of the horizontal axis is located at the center of the grid net. The results show three major aftershock alignments. Aftershocks are mainly distributed along two parallel planes dipping westward with a dip of about 50 degrees. We estimated that shallower (M) and deeper (A) alignments correspond to the fault plane of the main shock and that of the largest aftershock, respectively. In the central part, aftershocks are also distributed along a plane dipping to the ESE with a dip of about 40 degrees. They (B) are located mainly to the east of and below the fault plane of the largest aftershock and further extend to the shallower area between the fault planes of the main shock and the largest aftershock. This alignment probably corresponds to the fault plane of the M6 aftershock which occurred on October 27, 4 days after the mainshock. Another aftershock alignment (C) on an eastward dipping plane can be seen near the main shock hypocenter. They seem to extend to the hypocenter of the largest aftershock (Y~0km).

General feature of the estimated seismic velocity structure ( $V_p$  and  $V_s$ ) that the hanging wall (western part of the focal area) has the lower velocity and footwall (eastern part of the focal area) has higher velocity can be seen in all of these vertical cross sections. In the southern part (Y ~ -8km), uppermost portion with  $V_p$  of less than 5.0 km/s is distributed down to about a depth of 5km depth. In this area, aftershocks are composing two separate groups and the eastern group of aftershocks distributes along a plane where seismic velocity changes abruptly. Shallower extension of this plane seems

to meet the northern extension of the surface trace of the Muikamachi Fault ( $X \sim 6\text{km}$ ). In the central part ( $Y = -6\text{km} - +4\text{km}$ ), the uppermost portion with  $V_p$  of less than 5.0 km/s become thinner in comparison with in southern part and is distributed at depths shallower than a few km depth. The boundary between the low-velocity hanging wall and the high-velocity footwall (corresponding to the contour of  $V_p$  of about 6 km/s) seems to shift westward in comparison to in northern and southern parts, where the mainshock hypocenter was located ( $Y \sim -4\text{km}$ ). Aftershocks near the main shock fault plane (M) are distributed along a zone where seismic velocity changes abruptly, though aftershocks near to the fault plane of the largest aftershock (A) are also distributed along another zone where seismic velocity changes. Shallower extension of the aftershock alignment on the estimated main shock fault plane approximately meets the northern extension of the surface trace of the Suwatoge flexure and/or the Obiro Fault ( $X \sim 0\text{km}$ ), and the shallower extension of the aftershock alignment on the estimated largest aftershock fault plane meets the northern extension of the surface trace of the Muikamachi Fault. Aftershocks probably delimiting the fault plane of the largest aftershock are distributed along the zone where seismic velocity changes. An exception for this is the area around  $X = 0\text{km}$ , where the aftershocks are distributed along a narrow low-velocity zone. Aftershocks on the fault plane of the M6 aftershock on Oct. 27 (B) are also distributed along a narrow low-velocity zone.

#### Discussion & Conclusions

General feature of the obtained velocity structure is that the hanging wall (western part of the focal area) has lower velocity and the footwall (eastern part of the focal area) has higher velocity. Other tomographic studies also show similar features in the focal area of the present earthquake (Kato et al., 2005, Korenaga et al., 2005). Aftershocks are distributed along zones where seismic velocity changes rather abruptly. This feature is the same as that in the focal area of the 2003 northern Miyagi earthquake (Okada et al., 2004a). This is consistent with the Bouguer gravity anomaly distribution in this region (Honda and Kono, 2004) (gray contour line in Fig. 2). Higher velocity was obtained where the gravity anomaly is higher. Part of this velocity and gravity boundaries are almost correspond with Muikamachi fault, which is a part of the Shibata-Koide tectonic line (Kim, 2004, Kim and Okada, 2005). These faults acted as normal faults in the Miocene and were reactivated as reverse faults under the current compressional stress regime. These observations strongly suggest that the 2004 mid Niigata prefecture earthquake sequence occurred along the pre-existing faults, and it was strongly controlled by the pre-existing structure (e.g. Hirata et al., 2005, Sato and Kato, 2005).

We have successfully imaged some portions of fault planes of the present earthquake as low-velocity zones. Okada et al. (2005) also detected a low- $V_p$  and low- $V_s$  zone along the fault plane of the 1995 southern Hyogo (Kobe) earthquake. (Thurber et al., 1997, 2003) imaged a low- $V_p$  and high- $V_p/V_s$  zone, possibly corresponding to inclusions of water, down to a depth of about 3km within the fault zone of San Andreas Fault. Li et al. (2004) also showed low velocity ( $V_s$ ) zone along the fault zone by fault zone trapped waves. These low- $V_p$  and low- $V_s$  zones probably show the existence of highly fractured-damaged zones.

The low-velocity zone beneath the mainshock hypocenter seems to extend to the deeper part, although the resolution in the deeper part ( $Z > 12\text{km}$ ) is poor. This might image the upwelling fluid from the deeper part of the crust, which promotes deformation of crust and occurrence of the present earthquake as in the cases of other shallow inland earthquakes in NE Japan (Hasegawa et al., 2004).

We compared the seismic velocity distribution obtained in this study with the slip distribution by Yagi (2005) because he estimated from both the inversions of local and teleseismic seismograms and the hypocenter location of the present earthquake determined by his waveform inversion is almost the same as that in this study. Two asperities of the main shock rupture are estimated by Yagi (2005): One is located at a deeper part near the main shock hypocenter, and the other is located at a shallower part to the east of the hypocenter. The existence of one asperity near the hypocenter is consistent with other studies (e.g. Honda et al., 2005, Koketsu et al., 2005), though the slip distributions by Yagi are different from those reported by other researchers because they selected different data sets and different seismic velocity structure for calculating Green's function and so on. A comparison between the P-wave velocity distribution presented in this study and the slip distribution by Yagi (2005) shows that large slip areas (asperities) seem to be distributed along zones where P-wave velocity either changes abruptly or is relatively high, avoiding marked low-velocity areas which extend to a shallower part from the aftershock alignment of the M6 aftershock on Oct. 27 (e.g.  $Y \sim 2\text{km}$ ). This observation is consistent with the correspondence between high-velocity bodies and asperities reported in the previous studies: the 2003 northern Miyagi earthquake (M6.4) in NE Japan (Okada et al., 2004a-b), the 2000 western Tottori earthquake (M7.3) in SW Japan (Okada et al., 2004c), the 1995 southern Hyogo (Kobe) earthquake (Okada et al., 2005), the 2001 Geiyo intraslab earthquake in SW Japan

(Suganomata et al., 2004) and the 1966 Parkfield, California earthquake (Eberhart-Phillips and Michael, 1993).

In conclusions, after the 2004 mid Niigata prefecture earthquake occurred, we swiftly deployed a dense temporary seismic network for aftershock observation just above and around the focal area. Precise aftershock distribution and 3D seismic velocity structure in and around the fault planes of the earthquake and four major ( $M \geq 6$ ) aftershocks by applying the double-difference tomography method to this aftershock observation data show the following results. Aftershock distribution forms three major alignments. Two of them are almost parallel and dipping toward the WNW; the shallow aftershock alignment corresponds with the fault plane of the mainshock, and the deep one corresponds with that of the largest aftershock (M6.4). The third alignment is almost perpendicular to the WNW-ward dipping planes, and it is presumable that this corresponds with the fault plane of the M6 aftershock on Oct. 27. The hanging wall (western part of the focal area) has lower seismic velocity and the footwall (eastern part of the focal area) has higher velocity ( $V_p > \text{about } 6\text{km/s}$ ). The results also indicate that major velocity boundary shifts westward in comparison to in northern and southern parts at a location near the hypocenter of the main shock in the central part of the focal area; and that some part of the fault planes (e.g. M6 aftershock on Oct. 27) were imaged as low velocity zones.

#### Acknowledgments

We would like to express our condolences with people in the focal area of the 2004 mid Niigata prefecture earthquake on the disasters caused by the event. We are grateful for all the help by the organizations, municipalities, and people in the focal area of the present earthquake at the deployment. We borrowed some instruments from Kyoto Univ., Hirosaki Univ. and Yamagata Univ. Dr. Y. Iio of Kyoto Univ., Dr. M. Kosuga and Dr. K. Watanabe of Hirosaki Univ., and Prof. A. Hasemi of Yamagata Univ. kindly prepared and offered the instruments just after the occurrence of the main shock. We used data from Univ. of Tokyo, JMA, Hi-net, F-net, NIED. Discussions with Emeritus Prof. Y. Kono, Dr. R. Honda, Dr. Y. Hiramatsu of Kanazawa Univ., Dr. H. Kim of Kyoto Univ., and Dr. Y. Yagi of BRI were valuable. We would like to thank Prof. N. Hirata, Dr. Y. G. Li and Dr. S. Kodaira for helpful comments. This work was conducted under the support of Grant-in-Aid for Special Purposes (No. 16800054), MEXT, Japan. This work was also conducted as part of the 21st COE program, 'Advanced Science and Technology

Center for the Dynamic Earth', at Tohoku University. This work was also partially supported by MEXT.KAKENHI (16740247) and JSPS.KAKENHI (15204037), Japan.

## References

- Eberhart-Phillips, D. and A. Michael, Three-dimensional velocity structure, seismicity, and fault structure in the Parkfield Region, Central California, *J Geophys Res*, **98**, 15737-15758, 1993
- F-Net, NIED, NIED CMT solutions, <http://www.fnet.bosai.go.jp>, 2005
- Hasegawa, A., J. Nakajima, N. Umino, S. Miura and Y. Suwa, Crustal deformation and shallow seismic activity beneath the northeastern Japan arc (in Japanese with English abstract), *J Seism Soc Japan (Zisin)*, **56**, 413-424, 2004
- Hasegawa, A., N. Umino and A. Takagi, Double-planed structure of the deep seismic zone in the northeastern Japan arc, *Tectonophys*, **47**, 43-58, 1978
- Hirata, N., H. Sato, S. Sakai, A. Kato and E. Kurashimo, Fault system of the 2004 Mid Niigata prefecture earthquake and its aftershocks, *Landslides*, 2(2), doi:10.1007/s10346-005-0050-8, 2005
- Honda, R., S. Aoi, N. Morikawa, H. Sekiguchi, T. Kunugi and H. Fujiwara, Ground motion and rupture process of the 2004 mid Niigata prefecture earthquake obtained from strong motion data of K-NET and KiK-net, *Earth, Planets, and Space / Special section for the 2004 Mid Niigata Prefecture Earthquake*, submitted. 2005
- Honda, R. and Y. Kono, Gravity anomaly in the focal area of the 2004 Niigata Chuetsu earthquake, [http://hakusan.s.kanazawa-u.ac.jp/2gata/grav\\_niigata.html](http://hakusan.s.kanazawa-u.ac.jp/2gata/grav_niigata.html) (on Feb 15, 2005), 2004
- Kato, A., E. Kurashimo, N. Hirata, T. Iwasaki and T. Kanazawa, Imaging the source region of the 2004 Mid-Niigata prefecture earthquake and the evolution of a seismogenic thrust-related fold, *Geophysical Research Letters*, 32, L07307, doi:10.1029/2005GL022366, 2005
- Kim, H.Y., Relationship between the unheaval process of the Uonuma Hills and cumulative nature of the Muikamachi fault, central Japan, *Active Fault Research*, 24, 63-75, 2004
- Kim, H.Y. and A. Okada, Surface deformations associated with the October 2004 Mid-Niigata earthquakes: Description and discussion, *Earth, Planets, and*



- Space / Special section for the 2004 Mid Niigata Prefecture Earthquake*, submitted. 2005
- Kim, H.Y., A. Okada and H. Tsutsumi, 2004 Oct. Middle Niigata earthquake (Mj6.8): the surface earthquake faults generated in the Shinano river active fold and thrust zone, central Japan, *Hokudan 2005 International Symposium on Active Faulting*, 18201. 2005
- Kissling, E., W. Ellsworth, D. Eberhart-Phillips and U. Kradolfer, Initial reference models in local earthquake tomography, *J Geophys Res*, **99**, 19635-19646, 1994
- Koketsu, K., K. Hikima, H. Miyake and H. Tanaka, Source process and strong motions of the 2004 Niigata-Chuetsu earthquake (on 15/2/2005), <http://taro.eri.u-tokyo.ac.jp/saigai/chuetsu/chuetsu.html>, 2005
- Korenaga, M., S. Matsumoto, Y. Iio, T. Matsushima, K. Uehira and T. Shibutani, Three dimensional velocity structure around aftershock area of the 2004 Niigata-ken Chuetsu Earthquake (M6.8) by Double-Difference tomography, *Earth, Planets, and Space / Special section for the 2004 Mid Niigata Prefecture Earthquake*, submitted. 2005
- Li, Y.G., J.E. Vidale and S.E. Cochran, Low-velocity damaged structure of the San Andreas fault at Parkfield from fault-zone trapped waves, *Geophysical Research Letters*, 31, L12S06. 2004
- Okada, T., A. Hasegawa, J. Suganomata, N. Umino, H. Zhang and C. Thurber, Imaging the fault plane and asperities of the 2003 M6.4 northern Miyagi earthquake, NE Japan, by double-difference tomography, *Earth Planet Sci Lett*, submitted. 2004a
- Okada, T., A. Hasegawa, J. Suganomata, N. Umino, H. Zhang and C. Thurber, Imaging the fault plane of the 2003 M6.4 northern Miyagi, NE Japan, earthquake by double-difference tomography, *Eos Trans AGU, West Pac Geophys Suppl*, **85**, S42-A21, 2004b
- Okada, T., A. Hasegawa, J. Suganomata, D. Zhao, H. Zhang and C. Thurber, Imaging the fault plane and asperities of the 1995 southern Hyogo (Kobe) earthquake (M7.3) using double-difference tomography, *Geophysical Research Letters*, submitted. 2005
- Okada, T., A. Hasegawa, H. Zhang and C. Thurber, Detailed seismic velocity structure around the focal area of the 2000 Western Tottori earthquake (M7.3) by Double-Difference tomography, *2004c Japan EPS Joint Meeting*, J078-P001, 2004
- The Research Group for Active Fault in Japan, *Active faults in Japan* (2nd edition).

- Univ. Tokyo Press, Tokyo, 1991
- Sakai, S., S. Hashimoto, M. Kobayashi, K. Sakai, T. Haneda, T. Urabe and S. Tsukada, Aftershock distribution of the 1995 northern Niigata earthquake (M6.0) (in Japanese), *Chukyu Monthly*, **17**, 779-783, 1995
- Sato, H. and N. Kato, Relationship between the geologic structure and source fault of the 2004 Mid-Niigata prefecture earthquake, central Japan, *Earth, Planets, and Space / Special section for the 2004 Mid Niigata Prefecture Earthquake*, submitted. 2005
- Suganomata, J., T. Okada, A. Hasegawa, H. Zhang and C. Thurber, Heterogeneous seismic velocity structure in and around the source region of the 2001 M6.7 Geiyo intraslab earthquake, SW Japan, revealed by double-difference tomography, *Eos Trans AGU, West Pac Geophys Meet Suppl*, **85**, T23A-T270, 2004
- Thurber, C. and D. Eberhart-Phillips, Local earthquake tomography with flexible gridding, *Comp & Geosci*, **25**, 809-818, 1999
- Thurber, C., S. Roecker, W. Ellsworth, Y. Chen, W. Lutter and R. Sessions, Two-dimensional seismic image of the San Andreas Fault in the Northern Gabilan Range, central California: Evidence for fluids in the fault zone, *Geophysical Research Letters*, **24**, 1591-1594, 1997
- Thurber, C., S. Roecker, K. Roberts, M. Gold, L. Powell and K. Rittger, Earthquake locations and three-dimensional fault zone structure along the creeping section of the San Andreas fault near Parkfield, CA: Preparing for SAFOD, *Geophysical Research Letters*, **30**, 2002GL016004. 2003
- Yagi, Y., Source process of the 2004 Mid Niigata prefecture earthquake obtained by joint inversion of near-field and teleseismic, *Abstract for the 2005 Joint Meeting for Earth and Planetary Science, Japan*, s101p-s1001, 2005
- Zhang, H. and C. Thurber, Double-Difference Tomography: the method and its application to the Hayward Fault, California, *Bull Seism Soc Am*, **93**, 1875-1889, 2003

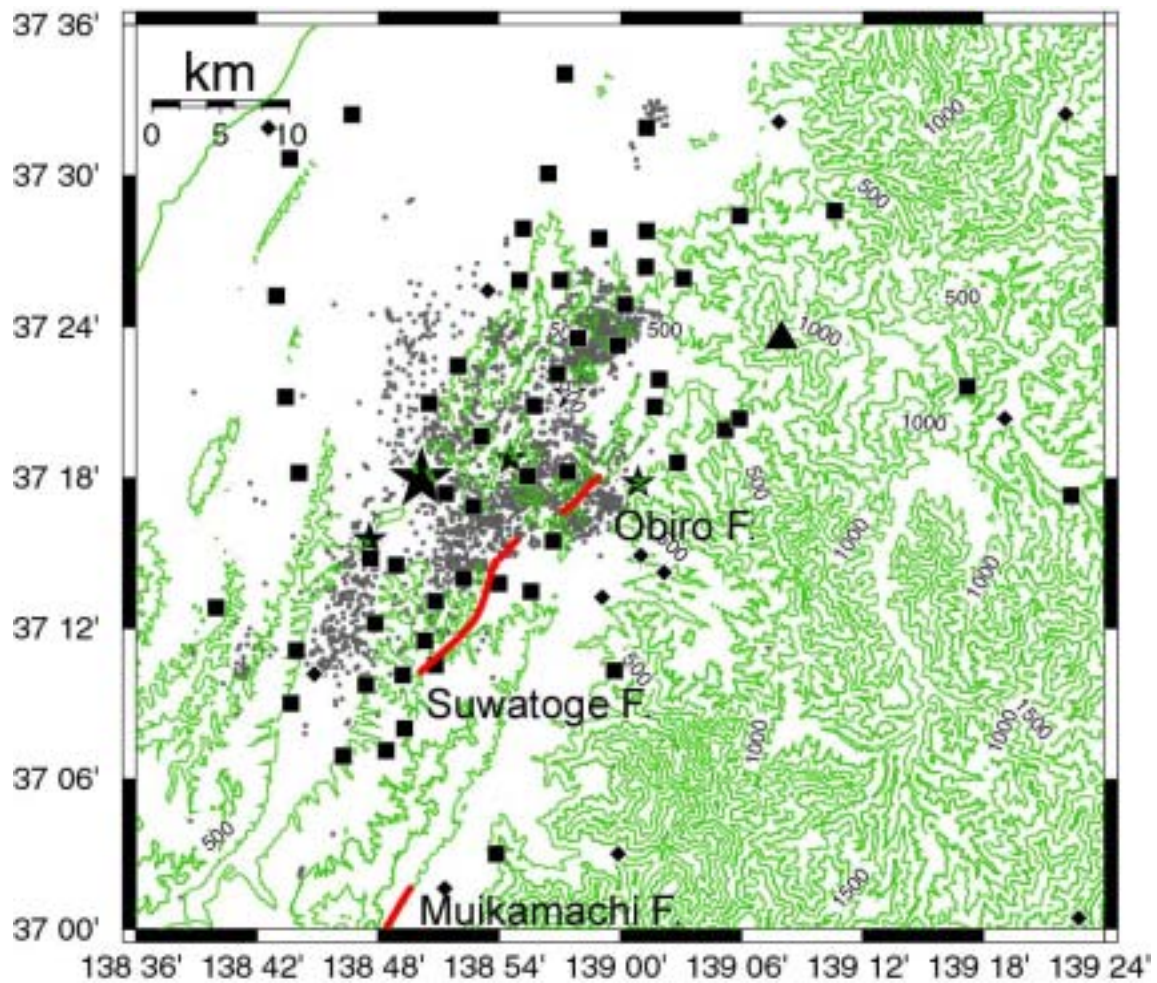


Fig. 1 Seismic stations used in this study. Square and diamond denotes temporary stations and the station operated routinely by ERI, Univ. of Tokyo, JMA and Hi-net, respectively. Large and small stars and dots denote epicenters of the main shock, aftershocks whose magnitude is greater than or equal to 6.0 and other aftershocks (27 Oct. 2004 – 21 Nov. 2004), respectively. Green contour lines show topography in an interval of 250m. Triangle denotes Sumon-dake volcano. Red bold lines show some of major active faults in and around the focal area of the present earthquake (Kim and Okada, 2005).

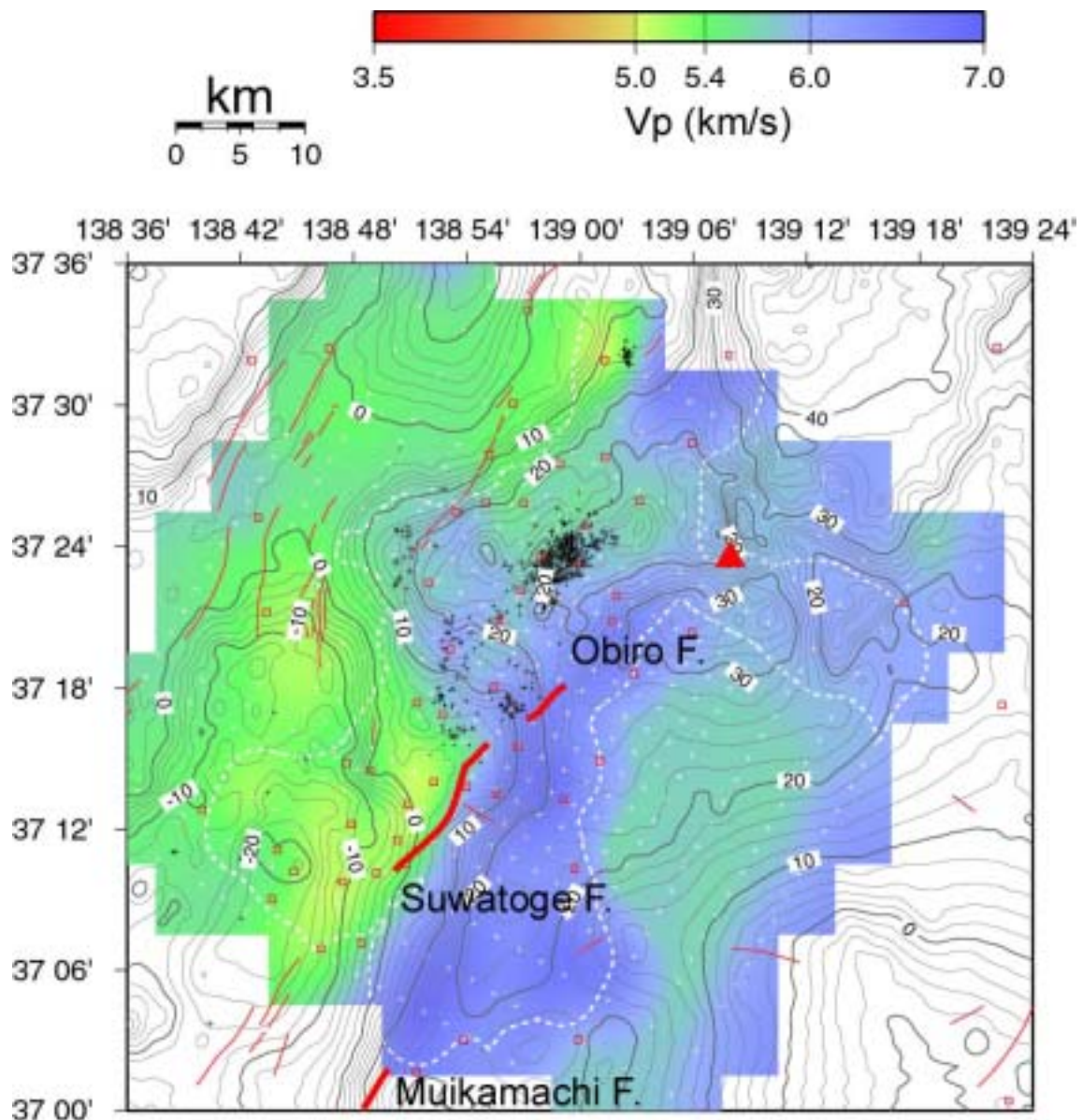


Fig. 2 Map view of P-wave velocity ( $V_p$ ) at a depth of 4km. Small black and white crosses and squares show epicenters of aftershocks at this depth, grids and seismic stations, respectively. DWS values are greater within the area shown by white broken lines, where reliable solutions were obtained. Bold and thin red lines show some major and other active faults, respectively (The Research Group for Active Fault in Japan, 1991, Kim and Okada, 2005). Gray contour lines show gravity (Bouguer) anomaly by (Honda and Kono, 2004). Red triangle shows Sumon-dake volcano.

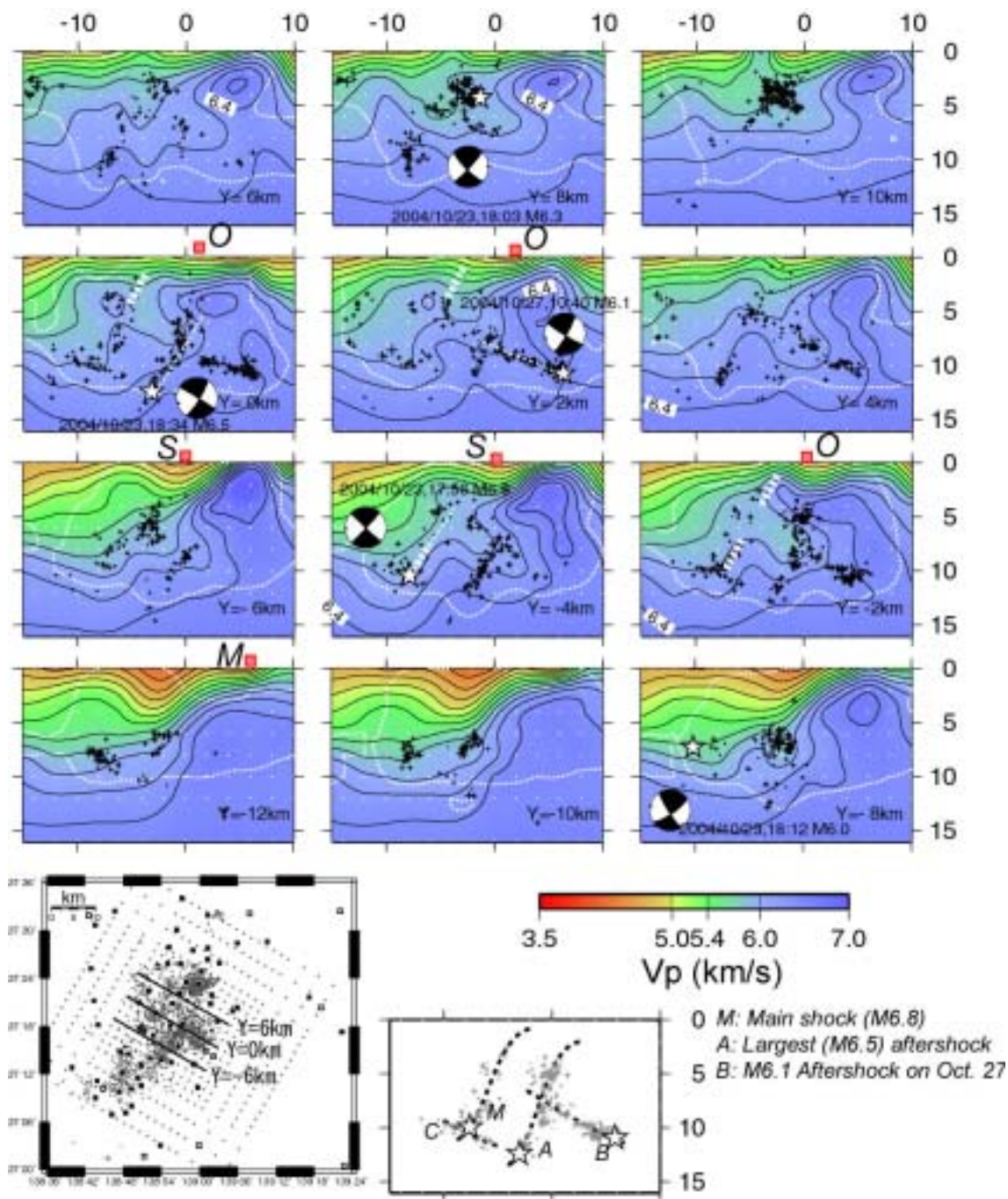


Fig. 3 Cross-fault vertical cross sections of P-wave velocity. Small black and white crosses show hypocenters of aftershocks and grids, respectively. DWS values are greater within the area shown by white broken lines. Large stars and small black crosses denotes hypocenters of the main shock, aftershocks whose magnitude is greater than or equal to 6.0 and other aftershocks (27 Oct. 2004 – 21 Nov. 2004), respectively. Moment tensor solutions by the F-net, NIED are also shown by lower hemisphere projection on the section. Thin white broken lines from stars show plausible fault planes of the main

shock, the largest aftershock and the M6 aftershock on Oct. 27. Thick white broken lines show large slip areas (asperities) of the main shock by (Yagi, 2005). Red boxes show surface traces of major active faults (M: Muikamachi, S: Suwatoge, O: Obiro). *Right-bottom figure shows schematic presentation of some major aftershock alignments (see text for details).*

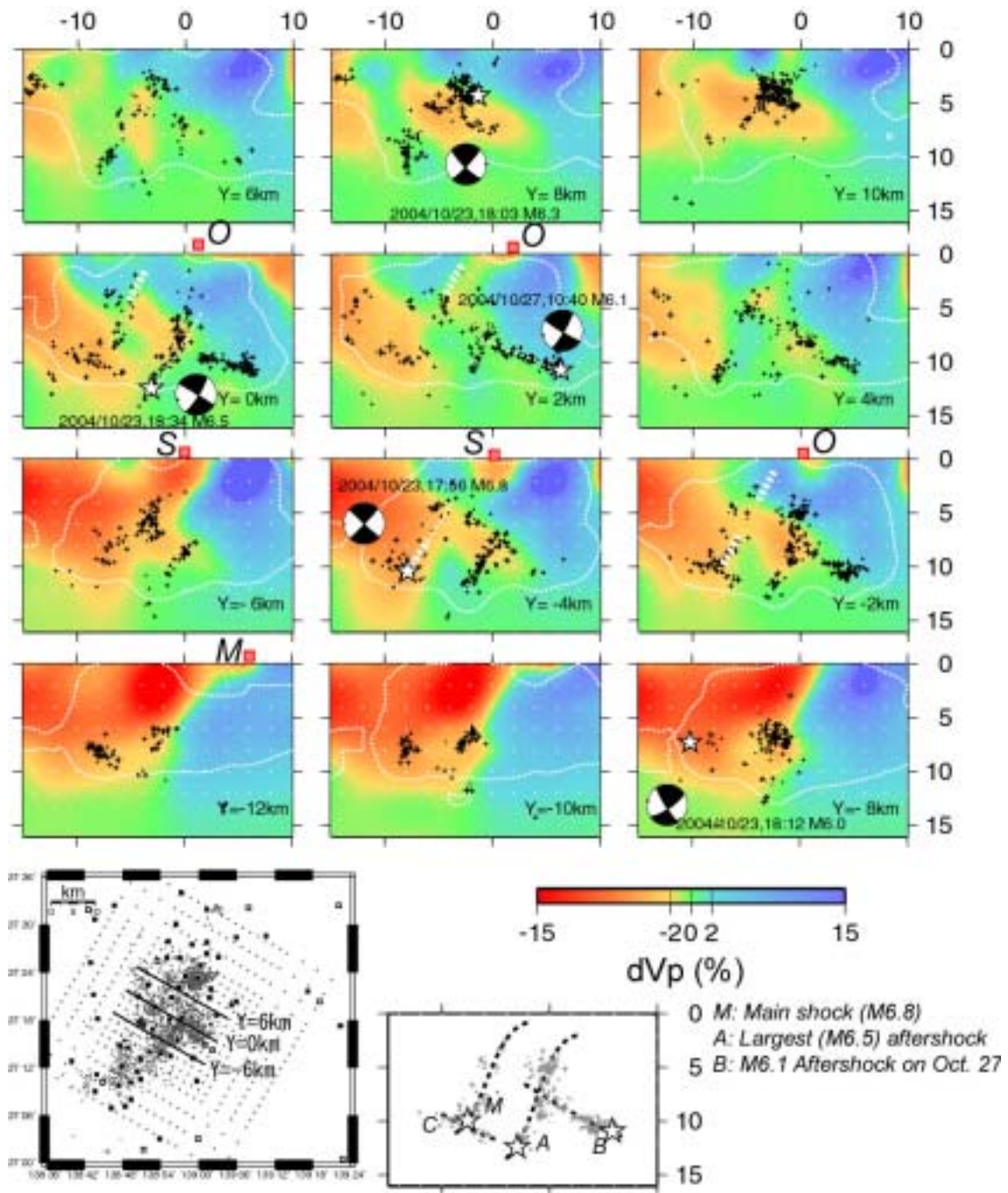


Fig. 4 Across-fault vertical cross sections of P-wave velocity perturbations from the average velocity at each depth.